

University of Wollongong

Research Online

Faculty of Engineering and Information
Sciences - Papers: Part A

Faculty of Engineering and Information
Sciences

1-1-2013

Study of PDMS based magnetorheological elastomers

Tongfei Tian

University Of Wollongong

Xing Zhong Zhang

University of Wollongong, xingzhon@uow.edu.au

Weihua Li

University of Wollongong, weihuali@uow.edu.au

Gursel Alici

University of Wollongong, gursel@uow.edu.au

J Ding

Defence Science and Technology Organisation

Follow this and additional works at: <https://ro.uow.edu.au/eispapers>



Part of the [Engineering Commons](#), and the [Science and Technology Studies Commons](#)

Recommended Citation

Tian, Tongfei; Zhang, Xing Zhong; Li, Weihua; Alici, Gursel; and Ding, J, "Study of PDMS based magnetorheological elastomers" (2013). *Faculty of Engineering and Information Sciences - Papers: Part A*. 490.

<https://ro.uow.edu.au/eispapers/490>

Research Online is the open access institutional repository for the University of Wollongong. For further information contact the UOW Library: research-pubs@uow.edu.au

Study of PDMS based magnetorheological elastomers

Abstract

The fabrication of conventional magnetorheological elastomers (MRE) is usually taken more than 1 day because the conventional matrixes such as natural rubber and silicone rubber need long curing time to become solid state. This study presents a rapid method for fabricating MRE within 90 minutes by using poly(dimethylsiloxane) (PDMS) as the matrix thanks to the rapid curing of PDMS in high temperature. A total of four PDMS based MRE samples were fabricated. Their mechanical and rheological properties under both steady-state and dynamic loading conditions were tested with a parallel-plate rheometer. Additionally, the microstructures of the PDMS based MREs were also observed by SEM and compared with the silicone rubber based MRE.

Keywords

study, magnetorheological, pdms, elastomers

Disciplines

Engineering | Science and Technology Studies

Publication Details

Tian, T. F., Zhang, X., Li, W., Alici, G. & Ding, J. (2013). Study of PDMS based magnetorheological elastomers. *Journal of Physics*, 412 1-8.

Study of PDMS based magnetorheological elastomers

This article has been downloaded from IOPscience. Please scroll down to see the full text article.

2013 J. Phys.: Conf. Ser. 412 012038

(<http://iopscience.iop.org/1742-6596/412/1/012038>)

View [the table of contents for this issue](#), or go to the [journal homepage](#) for more

Download details:

IP Address: 130.130.37.84

The article was downloaded on 22/02/2013 at 08:58

Please note that [terms and conditions apply](#).

Study of PDMS based magnetorheological elastomers

T F Tian^{1,3}, X Z Zhang¹, W H Li¹, G Alici¹ and J Ding²

¹ School of Mechanical, Materials and Mechatronic Engineering, University of Wollongong, Wollongong, NSW 2522, Australia

² Defence Science and Technology Organization, Human Protection and Performance Division, 506 Lorimer Street Fishermans Bend, VIC 3207, Australia

E-mail: tt436@uowmail.edu.au

Abstract. The fabrication of conventional magnetorheological elastomers (MRE) is usually taken more than 1 day because the conventional matrixes such as natural rubber and silicone rubber need long curing time to become solid state. This study presents a rapid method for fabricating MRE within 90 minutes by using poly(dimethylsiloxane) (PDMS) as the matrix thanks to the rapid curing of PDMS in high temperature. A total of four PDMS based MRE samples were fabricated. Their mechanical and rheological properties under both steady-state and dynamic loading conditions were tested with a parallel-plate rheometer. Additionally, the microstructures of the PDMS based MREs were also observed by SEM and compared with the silicone rubber based MRE.

1. Introduction

Magnetorheological elastomers (MREs) are a group of smart materials where polarized particles are suspended in a non-magnetic solid or gel-like matrix [1]. These materials exhibit characteristics that their moduli can be reversely controlled by an external magnetic field. MREs have recently found a variety of applications, such as adaptive tuned vibration absorbers, dampers, sensors and so on [2-10].

MREs generally consist of three major components: magnetisable particles, matrix and additives. Iron particles are generally used as the filler material to fabricate MREs. Both natural rubber and silicone rubber are used as typical matrixes [11-12]. Additives are commonly used to adjust the mechanical and chemical properties or electrical performance of MR fluids [13-14] as well as MR elastomers [15]. Silicone oil is an additive to increase the gaps between the matrix molecules and to decrease the gaps between the conglutination of molecules. Apart from increasing the plasticity and fluidity of the matrix, the additives can average the distribution of internal stress in the materials, which makes them ideal for fabricating MRE materials [16].

Natural rubber is an elastomer. The purified form of natural rubber is the chemical polyisoprene which can also be produced synthetically. Heat is normally required to vulcanise silicone rubber. The silicone rubber and a vulcanising silicon sealant (at room temperature) are mixed with silicon oil to change its ductility. The silicon oil is selected on the basis of preliminary studies with different elastomers.

PDMS is one example of silicon rubber. The PDMS has a low surface tension and is capable of wetting most surfaces. The stability and chemical neutrality of the system also enables the adhesive to

³ To whom any correspondence should be addressed.

bond to the metals [17]. PDMS is the most widely used silicon-based organic polymer, and is particularly known for its unique properties such as curing at low temperatures, rapid curing at high temperature, deformation reversibility and, surface chemistry controllable by reasonably well-developed techniques. PDMS is optically clear, and, in general, is considered to be inert, non-toxic and non-flammable [18-20]. Previous studies have focused on the structural properties of PDMS [21] and the kinetic properties under crystallization from solution [22].

In this investigation, PDMS is used as the matrix of MREs and studied the mechanical properties of the new MREs. Carbonyl iron particles can easily blend into PDMS because of its liquid initial state, meanwhile, the rapid curing of PMDS under certain temperature provides a quick method to fabricate MREs.

2. Experimental

2.1. Materials and fabrication

The base and curing agent of PDMS, type Sylgard 184 (Dow Corning Pty. LTD) at weight ratio 10:1 were firstly mixed evenly to be used as the carrying matrix, and then added to the carbonyl iron particles, type C3518 (Sigma-Aldrich Pty. LTD) and stirred sufficiently. The iron particles' diameter is between 3 μm and 5 μm at normal distribution. The density of iron particles and PMDS are 7.86 g/cm^3 and 1.1 g/cm^3 , respectively. The final mixtures were placed in a vacuum chamber to eliminate bubbles in 30 min and were placed between two pieces of plastic paper and pressed to be membranes. Some small cylinders with 1 mm thickness were used to ensure the thickness of MREs is 1 mm. Then the mixture was left for curing in an oven at 100°C for 35 minutes and then cut by a punch to disks with 20 mm diameter. The total time to fabricate the PDMS was no more than 100 min, which saves lot of time than the conventional MREs made of natural rubber or silicone rubber that need more than 24 h to curing.

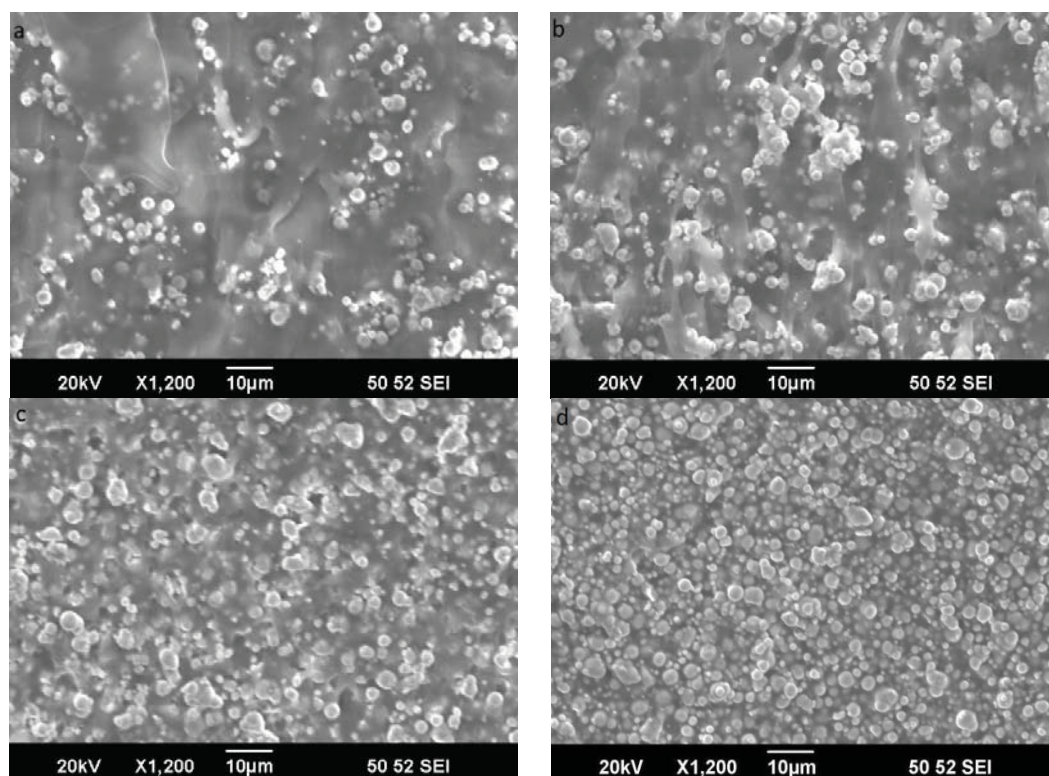


Figure 1. Microstructure of PDMS MREs (a) iron 60%, (b) iron 70%, (c) iron 80%, (d) iron 90%.

In this study, 4 PDMS MRE samples were fabricated whose iron particles' weight fraction (iron wt. %) were 60%, 70%, 80% and 90%. All MRE samples were isotropic.

2.2. Microstructure observation

LV-SEM (JSM 6490LV SEM) was used to observe the microstructure of PDMS MREs. Figure 1 shows the surface imaging for all MRE samples' microstructures and indicates that the carbonyl iron particles disperse randomly in the PDMS matrix due to the isotropy of all samples. The sample having higher iron weight fraction shows more iron particles in the same area.

2.3. Rheological measurement device

The shear-strain dependent rheology of the MREs was measured by a parallel-plate rheometer (MCR 301, Anton Paar, Germany). A Magneto Rheological Device (MRD 180, Anton Paar, Germany) was used to generate magnetic field in the test area and a temperature control device (Viscotherm VT2, Anton Paar, Germany) was used to control the measuring sample to be at 25 °C. Steady-state shear strain sweeps, dynamic strain sweeps, dynamic frequency sweeps and magnetic field intensity sweeps were carried out using the PP-20 measuring geometry (20 mm diameter) with a gap of 1 mm. The testing procedure for each measurement is illustrated below. Initially, the sample is sheared at a constant shear rate of 100 s⁻¹ at zero field for half a minute to distribute the particles uniformly. Next, the desired magnetic field is applied and maintained for more than 30 seconds so that the testing sample forms a static structure. Then, steady shear, dynamic oscillatory shear modes and, magnetic field intensity sweeps were employed to measure rheological properties of the samples under steady and dynamic loading conditions.

In this experiment, the magnetic flux density of the sample of MRE (BMRE) in the measuring gap depends not only on the current (I) applied to the samples and the magnetic properties of MRE materials. As the permeability of MRE samples varies little, an empirical equation, $BMRE = 220 I$, was employed to predict the flux density for different MRE samples, where the units of BMRE and I are in mT and amp (A), respectively. In the following test, the test current varies from 0 to 2 A with the increment 0.5 A, whose intensity of magnetic field is 0 to 440 mT with the increment 110 mT.

3. Results and discussion

3.1. Steady state

Under rotary shear the shear stress and strain of MREs under fields varying from 0~440 mT were measured at 25°C and 5 rad/s angular frequency. The shear rate range is from 0.0005 to 5 s⁻¹. The MR effect was evaluated by measuring the shear strain–stress curve of the sample with and without a magnetic field applied. Figure 2a–d shows the strain–stress curve of different samples at five different magnetic field intensities ranging from 0 to 440 mT. The slope of the strain–stress curve is the shear modulus of the material.

As can be seen in the figure 2a-d, all the samples' shear modulus show an increasing trend with magnetic field before they reach magnetic saturation at high field strength, which proves that all the MRE samples exhibit obvious MR effects. In figure 2d, it can be seen that the curve at 0 mT, which is the zero-field modulus of the 90 wt.% sample, shows a bigger slope of stress-strain curve compared with the lower graphite concentration samples, which means 90 wt.% sample has a higher zero-field modulus. When the strain is above the limitation, the shear stress reaches a saturation (maximum value) and decrease steadily. This might be due to the sliding effect. Additionally, other factors, such as the sample surface roughness and the normal force, could contribute to the resultant stress. In particular, they influence the static friction between the MRE sample and the upper plate, which consequently result in overshoots, as shown in figures 2a-d.

Also from figure 2a-d, the shear stress shows a linear relationship with the shear strain when the strain is within a range. This means that the MRE acts with linear viscoelastic properties when the

strain is below a limitation. Table 1 summarizes the linear ranges of all samples at various magnetic field intensities.

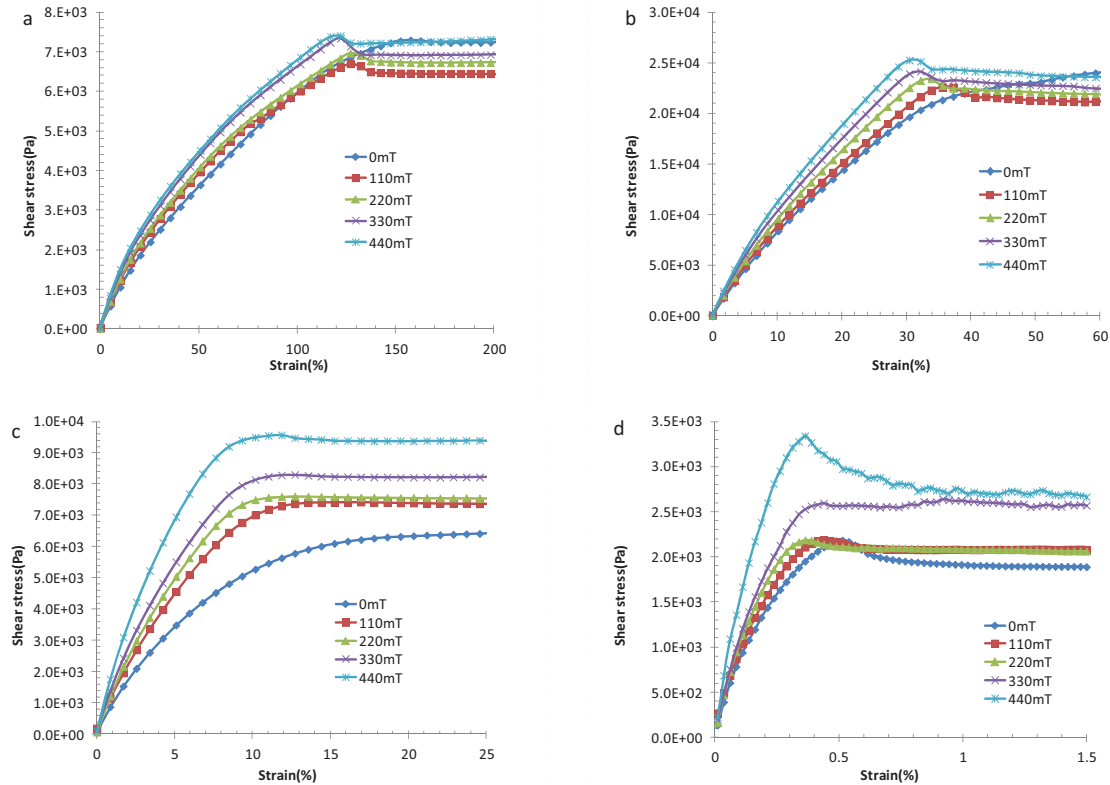


Figure 2. Strain-stress curve versus magnetic field (a) iron 60%, (b) iron 70%, (c) iron 80%, and (d) iron 90%.

Table 1. Linear range of all the samples at different magnetic fields.

Samples	Linear range				
	0mT	110mT	220mT	330mT	440mT
60% iron	150	127	127	123	120
70% iron	80	37	33	31	30
80% iron	40	10	9	9	8
90% iron	0.5	0.4	0.35	0.35	0.35

When the carbonyl iron weight fraction increases from 60% to 90%, the range of linearity decreases from 120%-150% to 0.35%-0.5%. The higher iron particles sample has the lower linear range. Meanwhile, the increasing magnetic field also contributes to the decreasing of the linear range.

3.2. Dynamic tests result

In order to obtain the dynamic mechanical behaviour of MRE, both strain amplitude sweep tests and angular frequency sweep tests were used. Five sets of data were collected for different amplitudes of oscillation, according to the various magnetic field inputs to the samples of MREs. Same as the steady state tests, five different magnetic field intensities, 0, 110, 220, 330 and 440 mT, were used in this experiment. The amplitude of shear strain in angular frequency sweep tests is set at 1% and the input frequency was 5 Hz in the strain amplitude sweep tests.

3.2.1. *Strain amplitude sweep.* In the strain sweep test, the storage and loss moduli were tested by varying strain from 0.1% to 100% at different magnetic fields and room temperature. Figure 3a-d shows the changing of storage modulus at the strain amplitude sweep.

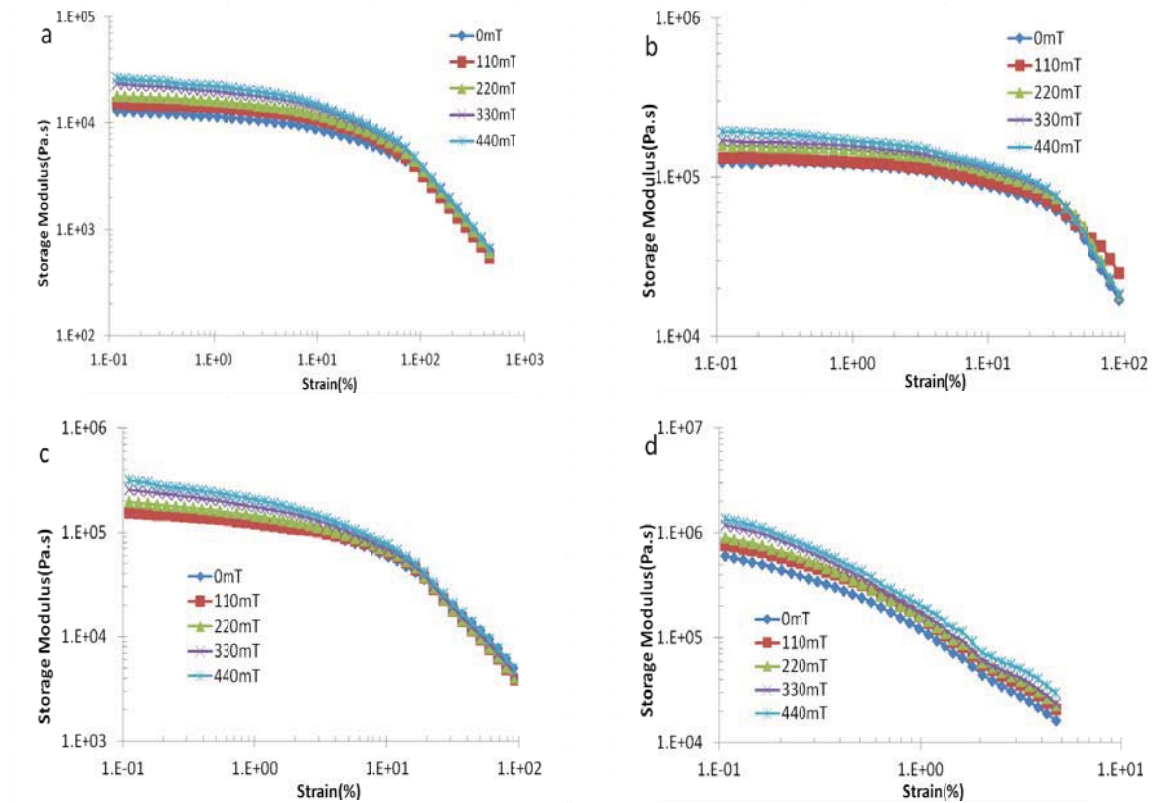


Figure 3. Storage modulus versus strain amplitude sweep (a) iron 60%, (b) iron 70%, (c) iron 80%, and (d) iron 90%.

In figure 3a-d, the overall trend of storage modulus is decreasing with the strain amplitude. It goes down smoothly within a critical shear strain and begins to drop significantly over the critical value and to go crossing with loss modulus, with which we can say that within the critical shear strain, the storage modulus shows approximately a linear relationship with the shear strain. Take sample containing 80% iron as an example, within 10% strain, its storage modulus versus strain as linear. These linear ranges are quite similar to the data in Table 1.

3.2.2. *Angular frequency sweep.* In this test, the strain is set at 1%. According to the experimental equipments, the angular frequency was varied from 1 to 100 s⁻¹ at different magnetic fields of 0, 110, 220, 330 and 440 mT. The figure 4a-d show the storage and loss moduli curves of the MRE samples under frequency sweep and at 25°C.

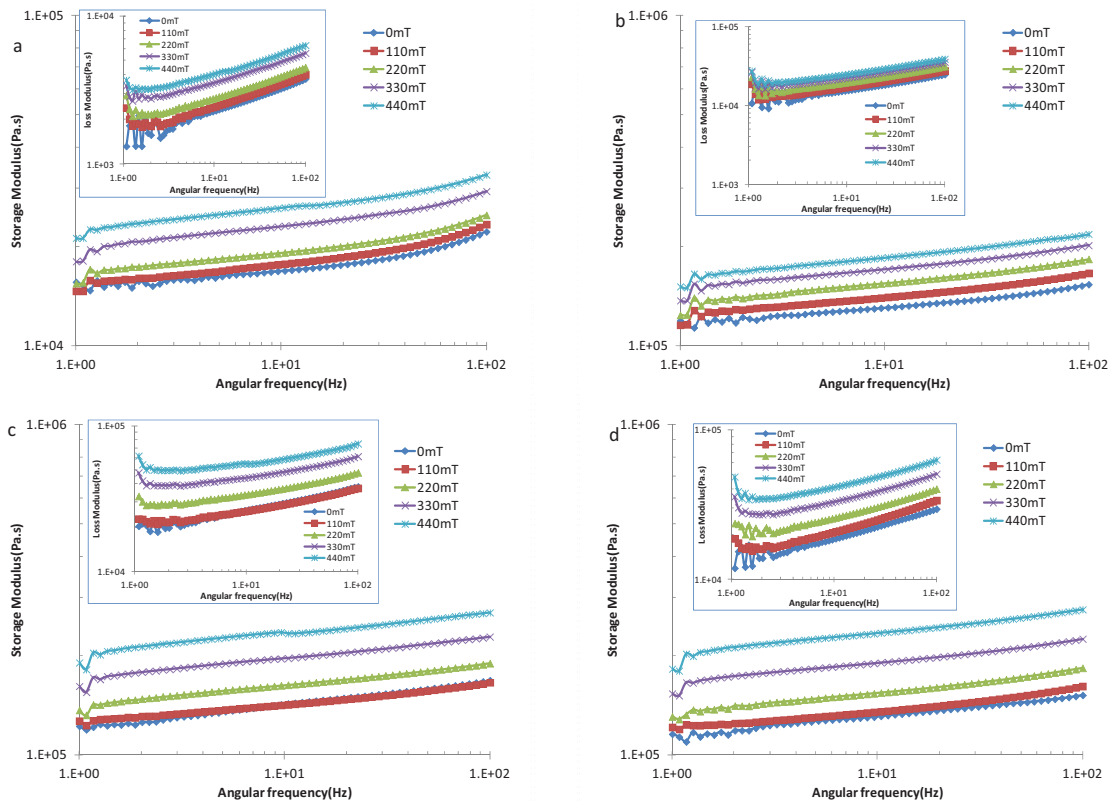


Figure 4. Storage and loss moduli versus angular frequency sweep (a) iron 60%, (b) iron 70%, (c) iron 80%, and (d) iron 90%.

From the figures above, we can see that in the log–log scale, the storage and loss moduli of all the samples are both increasing linearly with the growth of angular frequency. This means that at a higher angular frequency, the samples have bigger storage and loss moduli. This logarithmically linear relationship of the storage and loss moduli to the angular frequency can be used to predict the storage and loss moduli at a certain frequency.

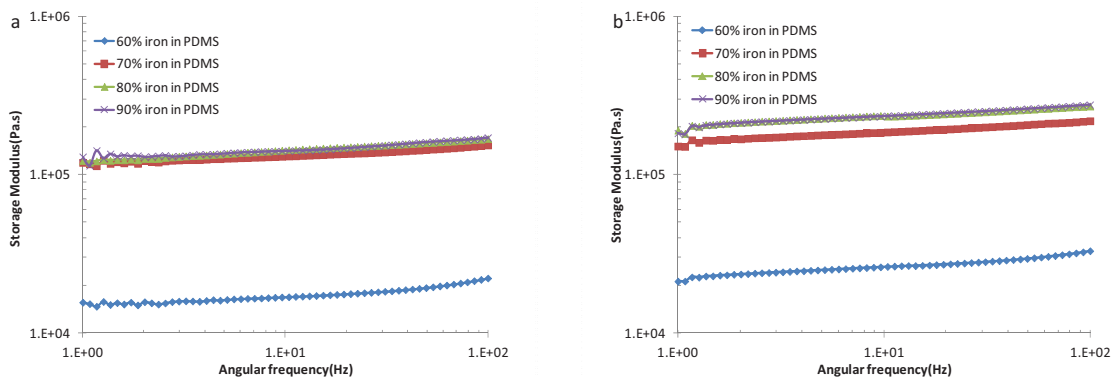


Figure 5. Storage modulus vs. angular frequency sweep (a) 0 mT and (b) 440 mT.

The effect of the iron weight fraction on the MR effect was shown in figure 5a-d. It can be seen from these figures that 60% iron sample has the lowest storage modulus, but the other three samples show very similar storage modulus at both low and high magnetic fields. This means that in PDMS

matrix, iron particles contribute to the MRE samples' initial stiffness before a critical weight fraction value between 60% and 70%, after which the stiffness of PMDS dominates in MREs' initial stiffness.

3.3. Magnetic field intensity sweep

The strain and angular frequency are set at 1% and 1 rad/s respectively, in this test. Magnetic field intensity is increasing from 0 mT to 440 mT linearly. This test is mainly used to figure out the relative MR effect (G'_{\max}/G'_0) of each sample. G'_0 denotes the MRE samples' zero-field storage modulus, G'_{\max} denotes the saturated field-induced modulus, and G'_{\max}/G'_0 denotes the relative MR effect. Figure 6a-b shows the storage modulus curves of the MRE samples versus magnetic field intensity at 25°C.

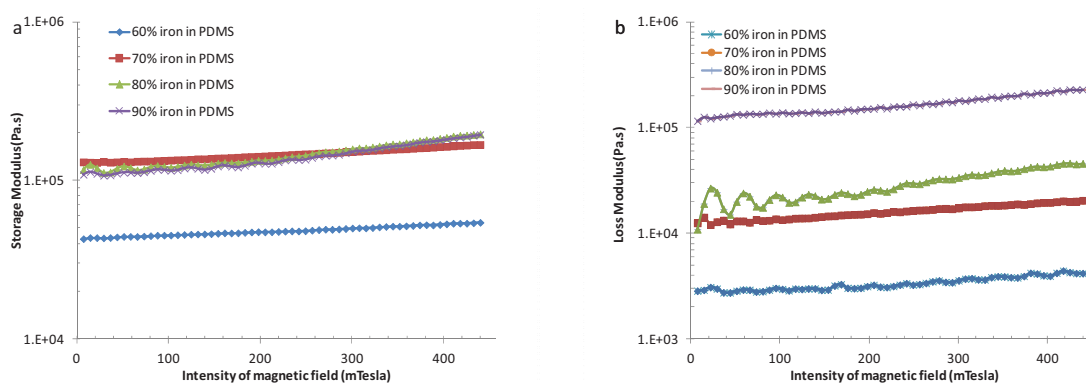


Figure 6. Storage and loss moduli vs. magnetic field intensity of different samples (a) Storage modulus and (b) Loss modulus.

From figure 6a we can see that the relative MR effect is 1.27, 1.30, 1.74 and 1.81 for 60%, 70%, 80% and 90% samples, respectively. The sample with higher iron particles concentration has higher relative MR effect. Also figure 6a shows the similar value of 70%, 80% and 90% sample, which proves that the mechanical properties of PMDS dominates in MREs' stiffness.

4. Conclusion

Four isotropic PDMS based MRE sample with 60%-90% iron particles weight fractions were fabricated in this study. The fabrication time for PDMS MREs is less than 100 min which is much shorter than the time needed for conventional MREs based on natural rubber or silicone rubber. LV SEM was used to observe their microstructures. This observation shows that iron particles disperse randomly in the isotropic samples.

The magnetic field intensity sweep, steady state and dynamic tests such as strain amplitude sweep and angular frequency sweep were used to test the magnetorheology of PDMS MREs. Because of the strong mechanical properties of PDMS, the storage and loss moduli are both changed less than the conventional MREs. The steady state tests showed that the increase of iron particles in the sample would diminish the viscoelastic linear range of MREs. The dynamic and magnetic field intensity sweep test proved that the samples with higher iron weight fraction show higher initial storage and loss moduli and also higher MR effects.

References

- [1] Ginder J M, Clark S M, Schlotter W F and Nichols M E 2002 *Int. J. Mod. Phys. B* **16** 2412–18
- [2] Deng H X, Gong X L and Wang L H 2006 *Smart Mater. Struct.* **15** 111-6
- [3] Ni Z C, Gong X L, Li J F and Chen L 2009 *J. Intell. Mater. Syst. Struct.* **20** 1195–202
- [4] Zhang X Z and Li W H 2009 *Smart Struct. Syst.* **5** 517–29
- [5] Kim Y K, Koo J H, Kim K S and Kim S H 2011 *Rev. Sci. Instrum.* **82** 035103
- [6] Xu Z B, Gong X L, Liao G J and Chen X M 2010 *J. Intell. Mater. Syst. Struct.* **21** 1039–47

- [7] Zhang W, Gong X L, Jiang W Q and Fan Y C (2010) *Smart Mater. Struct.* **19** 085008
- [8] Chen L, Gong X L and Li W H (2007) *Smart Mater. Struct.* **16** 2645–50
- [9] Li W H, Kostidis K, Zhang X Z, Zhou Y 2009 *Ieee/Asme Int. Conf. Advanced Intelligent Mechatronics* **1-3** 233–38
- [10] Bica I 2010 *J. Ind. Eng. Chem.* **16** 359–63
- [11] Gong X L, Zhang X Z and Zhang P Q 2005 *Polym. Test* **24** 669–76
- [12] Li W H, Zhou Y and Tian T F 2010 *Rheol. Acta.* **49** 733–40
- [13] Park B J, Song K H and Choi H J 2009 *Mater. Lett.* **63** 1350–52
- [14] Fang F F, Choi H J and Jhon M S 2009 *Colloids Surf. A* **351** 46–51
- [15] Zhang X Z, Peng S L, Wen W J and Li W H 2008 *Smart. Mater. Struct.* **17** 045001
- [16] Leblanc J L 2002 *Prog. Polym. Sci.* **27** 627–87
- [17] De Buyl F 2001 *Int. J. Adhes. Adhes.* **21** 411–22
- [18] Sundararajan PR 2002 *Polymer* **43** 1691-93.
- [19] McDonald J C, Duffy D C, Anderson J R, Chiu D T, Wu H K, Schueller O J A and Whitesides G 2000 *Electrophoresis* **21** 27-40.
- [20] Noonan K J T and Gates D P 2008 *Annu. Rep. Prog. Chem., Sect. A: Inorg. Chem.* **104** 394-413.
- [21] Rajan G S, Sur G S, Mark J E, Schaefer D W and Beaucage G 2003 *J. Polym. Sci., Part B: Polym. Phys.* **41** 1897-901.
- [22] Feio G, Buntinx G and Cohen-Addad J P 1989 *J. Polym. Sci., Part B: Polym. Phys.* **27** 1-24.